Time-Domain Beam Propagation Method and Its Application to Photonic Crystal Circuits

Masanori Koshiba, *Senior Member, IEEE*, Yasuhide Tsuji, *Member, IEEE*, and Masafumi Hikari

***Abstract*—A time-domain beam propagation method (BPM) based on the finite-element scheme is described for the analysis of reflections of both transverse electric and transverse magnetic polarized pulses in waveguiding structures containing arbitrarily shaped discontinuities. In order to avoid nonphysical reflections from the computational window edges, the perfectly matched layer boundary condition is introduced. The present algorithm using the Padé approximation is, to our knowledge, the first time-domain beam propagation method which can treat wide-band optical pulses. After validating this method for an optical grating with modulated refrative indexes, various photonic crystal circuit components are simulated.**

***Index Terms*—Finite-element method (FEM), optical waveguide analysis, photonic crystal, time-domain analysis, time-domain beam propagation method (TD-BPM).**

I. Introduction

THE BEAM propagation method (BPM) is at present the most widely used for the study of light propagation in longitudinally varying optical waveguides and now there are a great number of versions of BPM [1]. Especially, a recently developed BPM based on the finite-element method (FE-BPM) [2]–[5] using the Padé approximation [6] can give very accuate results without increasing computational effort even if the wide-angle beam propagation is treated. However, BPM assumes only the forward propagating waves, and thus, it is difficult to take into account backward reflecting waves. One method used to study distributed reflection and diffraction at arbitrary angle is the finite difference time-domain (FDTD) technique [7]. This technique is very powerful and versatile, and has been introduced and adapted to optical waveguide devices [8]–[10]. In FDTD very small time step size must be used because both the carrier and the modulated envelope are included in the wave propagator.

Recently, under the condition that the modulation frequency is much lower than the carrier frequency, a simple and efficient propagation algorithm in time domain has been developed and is called the time-domain BPM (TD-BPM) [11], [12]. In this new algorithm the computational spatial domain is discretized with the finite difference method (FDM), hereafter, referred to as FDTD-BPM. The removal of the fast carrier allows one to track a slowly varying envelope of a pulsed wave directly in time domain and thus, the converged solution could be obtained with moderate time step size. Despite its programming simplicity, it has suffered from the staircasing approximation when modeling curved geometries because in FDM, it is, in general, difficult to use nonuniform and nonorthogonal meshes. Furthermore, the formulation was limited to transverse electric (TE) modes and was based on the Fresnel or paraxial approximation. Therefore, the wide-band and/or transverse magnetic (TM)-pulsed wave propagation cannot be treated.

Manuscript received March 12, 1999; revised September 1, 1999.
The authors are with the Division of Electronics and Information Engineering, Hokkaido University, Sapporo 060-8628, Japan (e-mail: koshiba@ice.eng.hokudai.ac.jp).
Publisher Item Identifier S 0733-8724(00)01466-3.

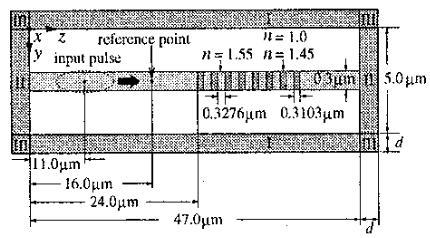

Fig. 1. Optical grating with modulated refractive indexes.

In this paper, a unified TD-BPM based on the finite-element method (FEM) abbreviated as FETD-BPM is described for both TE and TM polarized pulses propagating in arbitrarily shaped waveguiding structures. In order to avoid nonphysical reflections from the computational window edges, the perfectly matched layer (PML) boundary condition [5], [13] is introduced. The present algorithm using the Padé approximation is, to our knowledge, the first wide-band TD-BPM. After validating this method for an optical grating with modulated refractive indexes, numerical results are shown for a sharp bend, a T-branch, a Y-branch, a directional coupler, a multimode coupler, and a microcavity, all based on photonic bandgap (PBG) structures [14].

II. Basic Equation

We consider a two-dimensional (2-D) optical waveguide, where the computational window (domain) is on the yz-plane and there is no variation in the x direction. With these assumptions and the transversely scaled version of PML [5], [13] with artificial electric and magnetic conductivities of parabolic profile, we obtain the following basic equation:

$$s_y \frac{\partial}{\partial y}\left(p\,\frac{s_y}{s}\,\frac{\partial \Phi}{\partial y}\right) + s_z \frac{\partial}{\partial z}\left(p\,\frac{s_z}{s}\,\frac{\partial \Phi}{\partial z}\right) - s\,\frac{q}{c^2}\,\frac{\partial^2 \Phi}{\partial t^2} = 0 \quad (1)$$

with

$$\Phi = E_x, \quad p = 1, \quad q = n^2, \qquad \text{for TE modes} \quad (2)$$

$$\Phi = H_x, \quad p = 1/n^2, \quad q = 1, \qquad \text{for TM modes} \quad (3)$$

$$s = \begin{cases} 1 - j\,\dfrac{3c}{2\omega_0 n d}\left(\dfrac{\rho}{d}\right)^2 \ln\dfrac{1}{R}, & \text{in PML region} \\ 1, & \text{in non-PML region} \end{cases} \quad (4)$$

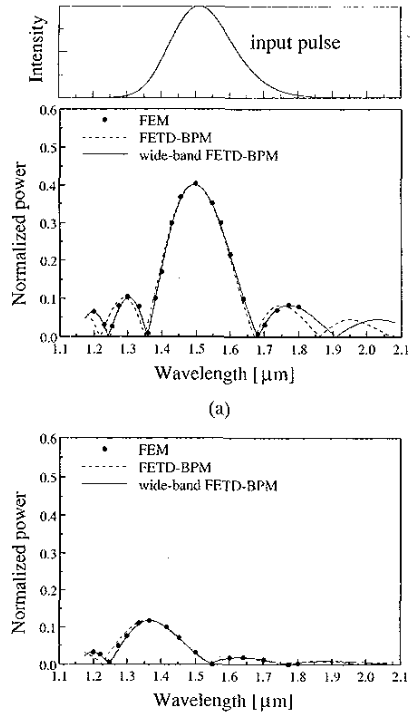

Fig. 2. Reflection characteristics of an optical grating for: (a) TE and (b) TM modes.

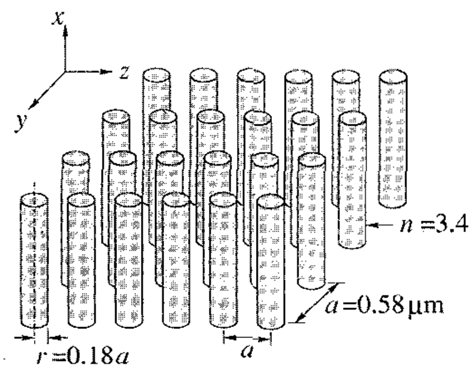

Fig. 3. Photonic crystal.

where

- E_x x components of the electric fields;
- H_x x components of the magnetic fields;
- t time;
- c speed of light in free space;
- n refractive index;
- ω_0 carrier center angular frequency;
- d PML thickness;
- ρ distance from the beginning of PML;
- R theoretical reflection coefficient [15].

For the PML regions I (perpendicular to the y axis), II (perpendicular to the z axis), or III (corners), $s_y = 1$ and $s_z = s$, $s_y = s$ and $s_z = 1$, or $s_y = s_z = 1$, respectively.

III. Finite Element Discretization

Substituting a solution of the form

$$\Phi(y,z,t) = \phi(y,z,t)\exp(j\omega_0 t) \tag{5}$$

into (1), we obtain the following equation for the slowly varying complex amplitude ϕ:

$$-s\frac{q}{c^2}\frac{\partial^2\phi}{\partial t^2} - 2js\frac{\omega_0 q}{c^2}\frac{\partial\phi}{\partial t} + s_y\frac{\partial}{\partial y}\left(p\frac{s_y}{s}\frac{\partial\phi}{\partial y}\right) + s_z\frac{\partial}{\partial z}\left(p\frac{s_z}{s}\frac{\partial\phi}{\partial z}\right) + s\frac{\omega_0^2 q}{c^2}\phi = 0. \tag{6}$$

Dividing the spatial domain into quadratic (second-order) triangular elements and applying the standard finite-element technique to (6), we obtain

$$-\frac{1}{c^2}[M]\frac{d^2\{\phi\}}{dt^2} - 2j\frac{\omega_0}{c^2}[M]\frac{d\{\phi\}}{dt} + \left([K] + \frac{\omega_0^2}{c^2}[M]\right)\{\phi\} = \{0\} \tag{7}$$

where

- $\{\phi\}$ global electric or magnetic field vector;
- $\{0\}$ null vector;

and the finite-element matrices are given by

$$[K] = \sum_e \iint_e \left[-p\frac{s_y^2}{s}\frac{\partial\{N\}}{\partial y}\frac{\partial\{N\}^T}{\partial y} - p\frac{s_z^2}{s}\frac{\partial\{N\}}{\partial z}\frac{\partial\{N\}^T}{\partial z}\right] dy\,dz \tag{8}$$

$$[M] = \sum_e \iint_e sq\{N\}\{N\}^T\,dy\,dz \tag{9}$$

where

- $\{N\}$ shape function vector;
- T denotes a transpose;
- $\sum_e$ extends over all different elements.

Utilizing the Padé recurrence relation [1]–[6], the following equation of TD-BPM (wide-angle FETD-BPM), which can treat wide-band optical pulses, is obtained:

$$-2j\frac{\omega_0}{c^2}[\tilde{M}]\frac{d\{\phi\}}{dt} + \left([K] + \frac{\omega_0^2}{c^2}[M]\right)\{\phi\} = \{0\} \tag{10}$$

with

$$[\tilde{M}] = [M] - \frac{c^2}{4\omega_0^2}\left([K] + \frac{\omega_0^2}{c^2}[M]\right). \tag{11}$$

The Fresnel or paraxial equation of TD-BPM (narrow band FETD-BPM, for simplicity, abbreviated as FETD-BPM) is easily obtained from (10) by replacing the matrix $[\tilde{M}]$ by $[M]$.

Applying the Crank–Nicholson algorithm for the time t to (10) yields

$$[A]_i\{\phi\}_{i+1} = [B]_i\{\phi\}_i \tag{12}$$

with

$$[A]_i = -2j\frac{\omega_0}{c^2}[\tilde{M}]_i + 0.5\Delta t\left([K]_i + \frac{\omega_0^2}{c^2}[M]_i\right) \tag{13}$$

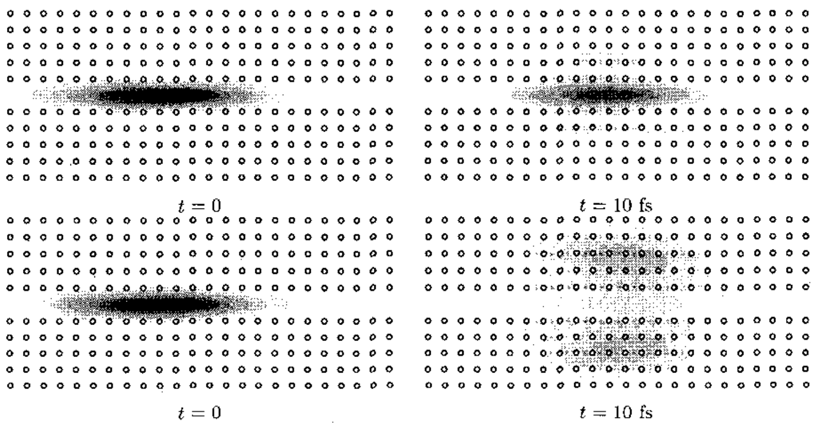

Fig. 4. Electric or magnetic field patterns in a straight waveguide for: (a) TE and (b) TM pulses.

$$[B]_i = -2j\,\frac{\omega_0}{c^2}\,[\tilde{M}]_i - 0.5\Delta t\left([K]_i + \frac{\omega_0^2}{c^2}\,[M]_i\right) \qquad (14)$$

where

Δt	time step size;
$\{\phi\}_i$	ith time steps;
$\{\phi\}_{i+1}$	$(i+1)$ time steps.

The Bi-CGSTAB algorithm [16] is introduced to solve the linear (12).

IV. Numerical Results

A. Optical Grating

We consider an optical grating as shown in Fig. 1, where the number of grating periods is eight and the PML thickness $d = 1.0$ μm. The input pulse with a transverse profile $\phi_0(y)$ corresponding to the fundamental mode of the planar waveguide and a Gaussian profile in the longitudinal direction at $t = 0$ is taken as

$$\phi(y, z, t = 0) = \phi_0(y)\,\exp\left[-\left(\frac{z - z_0}{W_0}\right)^2\right] \cdot \exp[-j\beta(z - z_0)] \qquad (15)$$

where

β	propagation constant;
z_0	center position of the input pulse;
W_0	spot size.

The reflected and transmitted pulses are monitored inside the waveguide. The fast Fourier transform of these pulses, normalized to the spectrum of the input pulse, gives the reflection and transmission spectra.

Fig. 2 shows the reflection characteristics with the input pulse spectrum, where $z_0 = 11.0$ μm, $W_0 = 2.0$ μm, the carrier center wavelength $\lambda_0 = 1.50$ μm. The time step size used is $\Delta t = 1.0$ fs which is, in general, sufficient to obtain stable solutions in the TD-BPM analysis [11]. The total duration simulated is 220 fs. On a DEC-alpha workstation (500 MHz), the code takes 25 MB of memory for 37 555 nodal points and 2 098 s to run. The input and reflected pulses are monitored at the reference point as in Fig. 1, and the reflected spectra are evaluated from the ratio between the Fourier transforms of the reflected pulse and the incident pulse. Although the accuracy of FETD-BPM may be limited to a narrow spectrum around the carrier center frequency ω_0, for both TE and TM modes, the results of wide-band FETD-BPM agree well with those of the conventional FEM formulated in frequency domain [17] over a wide range of frequencies, compared to the paraxial FETD-BPM. In the FEM [17] the reflection and transmission characteristics are calculated at every one frequency.

B. Photonic Crystal Circuits

Photonic crystals have inspired great interest recently because of their potential ability to control the propagation of light. Mekis *et al.* have demonstrated high transmission through sharp bends in photonic crystal waveguides [10].

We consider a photonic crystal of dielectric rods in air on a square array with lattice constant a [10] as shown in Fig. 3. The crystal has PBG for TE modes which extends from $\omega = 0.302 \times 2\pi c/a$ to $\omega = 0.443 \times 2\pi c/a$, but not for TM modes. Fig. 4 shows the electric field patterns of the pulse with Gaussian profiles in both the transverse and longitudinal directions propagating in a straight waveguide, where $\lambda_0 = 1.5$ μm and $\Delta t = 1.0$ fs. It is confirmed that the TE pulse is confined in the defect, core region, while the TM pulse cannot be guided and is radiated into the cladding region. In the following, therefore we consider the TE pulse propagatoin and the time step size is taken as $\Delta t = 1.0$ fs.

Fig. 5(a) shows a 90° bend proposed by Mekis *et al.* [10] and (b) the element division in the neighboorhood of the corner, and (c) the reflection and transmission characteristics. On a DEC-alpha workstation (500 MHz), the code takes 85 MB of memory for 158 607 nodal points and 106 s per time step of $\Delta t = 1.0$ fs to run. Two pulses with $\lambda_0 = 1.45$ μm (solid line) and $\lambda_0 = 1.65$ μm (dashed line) are sent down the waveguide covering different ranges of frequencies, and the input pulse at $t = 0$ fs is taken as

$$\phi(y, z, t = 0) = \phi_0(y, z)\,\exp\left[-\left(\frac{z - z_0}{W_0}\right)^2\right] \cdot \exp[-j\beta(z - z_0)] \qquad (16)$$

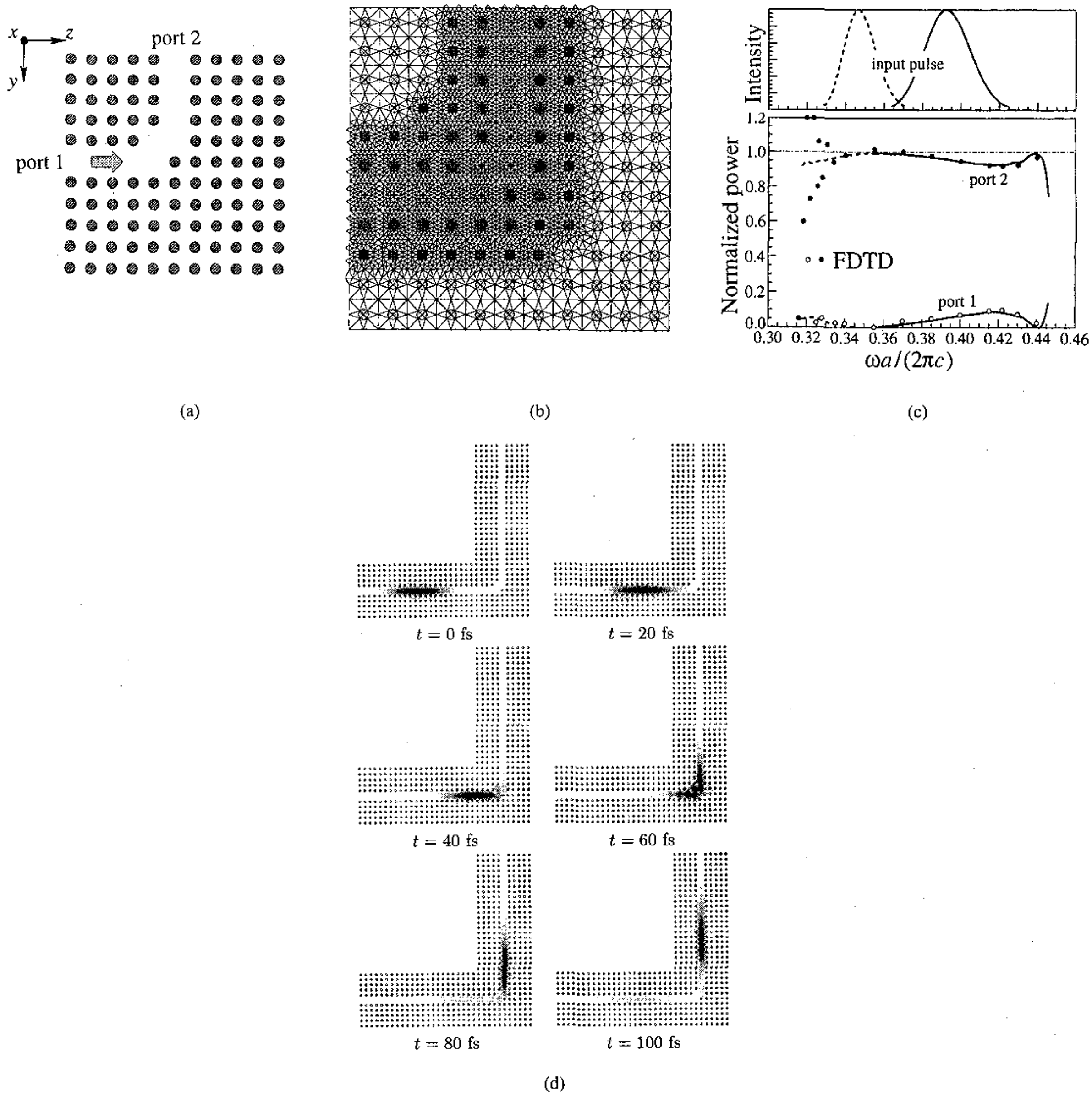

Fig. 5. 90° bend with (a) structure, (b) element division, (c) propagation characteristics, and (d) electric field patterns.

with

$$\phi_0(y,z) = \phi_0(y, z+ma), \qquad m = 0, \pm 1, \pm 2, \ldots \tag{17}$$

where $\phi_0(y,z)$ is a periodic function corresponding to the fundamental mode of the photonic crystal waveguide of period a. For all examples presented in connection with photonic crystal circuits in this subsection, the input pulses are the same. One is at $\lambda_0 = 1.45$ μm (solid line) and the other at $\lambda_0 = 1.65$ μm (dashed line) as shown in the top panel of Fig. 5(c). Also, for all propagation curves shown in Figs. 5–10, solid and dashed lines correspond to the input pulses at $\lambda_0 = 1.45$ μm and at $\lambda_0 = 1.65$ μm, respectively.

In Fig. 5(c) the results of FDTD using six pulses [10] are also plotted. In the FDTD calculation [10], nonphysical, spurious Gibbs oscillations are observed near the lower cutoff frequencies. On the other hand, such phenomena do not occur in our calculation. Fig. 5(d) shows the electric field patterns for the pulse of $\lambda_0 = 1.45$ μm. Fig. 6(a) shows a 90° bend with zero radius of curvature, (b) the reflection and transmission characteristics, and (c) the electric field patterns ($\lambda_0 = 1.45$ μm). The transmission is a little deteriorated.

Now, we propose photonic crystal circuit components as shown in Figs. 7–12 and simulate those propagation characteristics.

Fig. 7(a) shows a T-branch. From Fig. 7(b) high transmission is observed at frequency ranges from $\omega = 0.386 \times 2\pi c/a$ to $\omega = 0.403 \times 2\pi c/a$. From Fig. 8(a) and (b), on the other hand, we can see that the transmission property of a Y-branch is not so good because of high return loss. The electric field patterns ($\lambda_0 =$

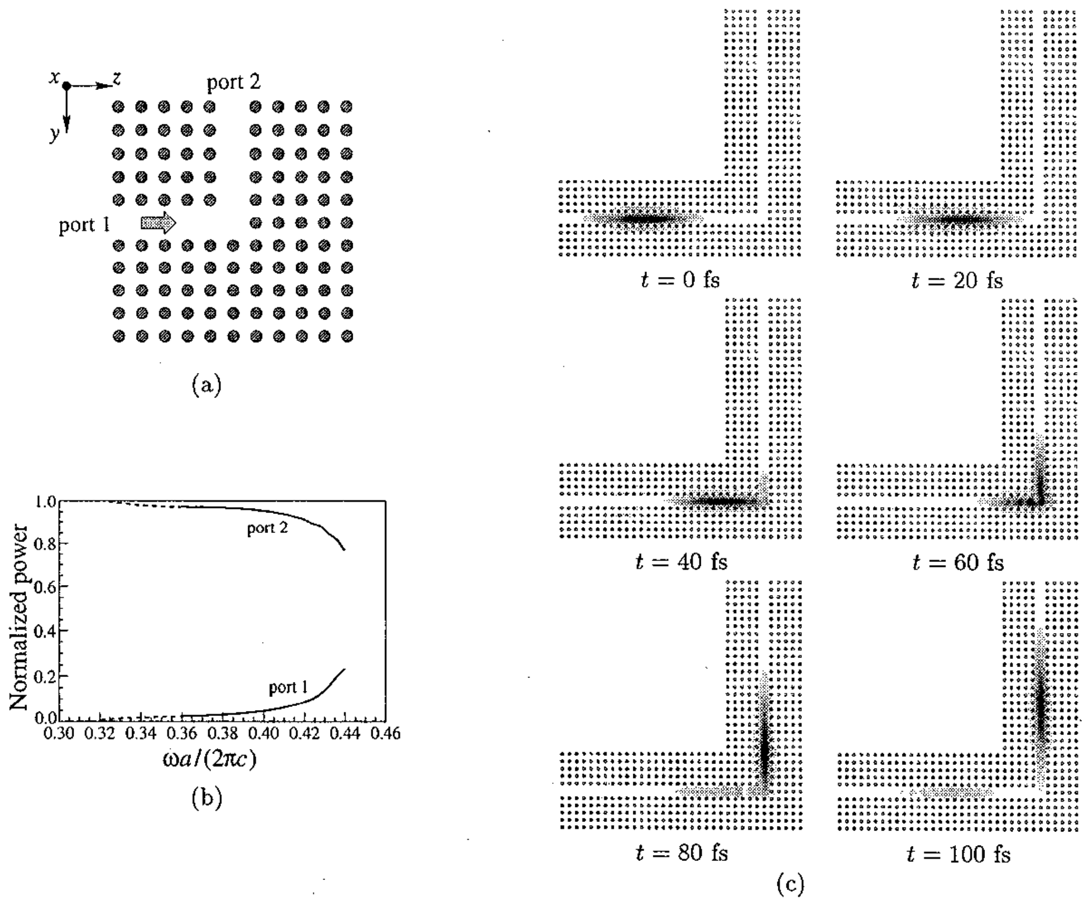

Fig. 6. Zero-curvature 90° bend with (a) structure, (b) propagation characteristics, and (c) electric field patterns.

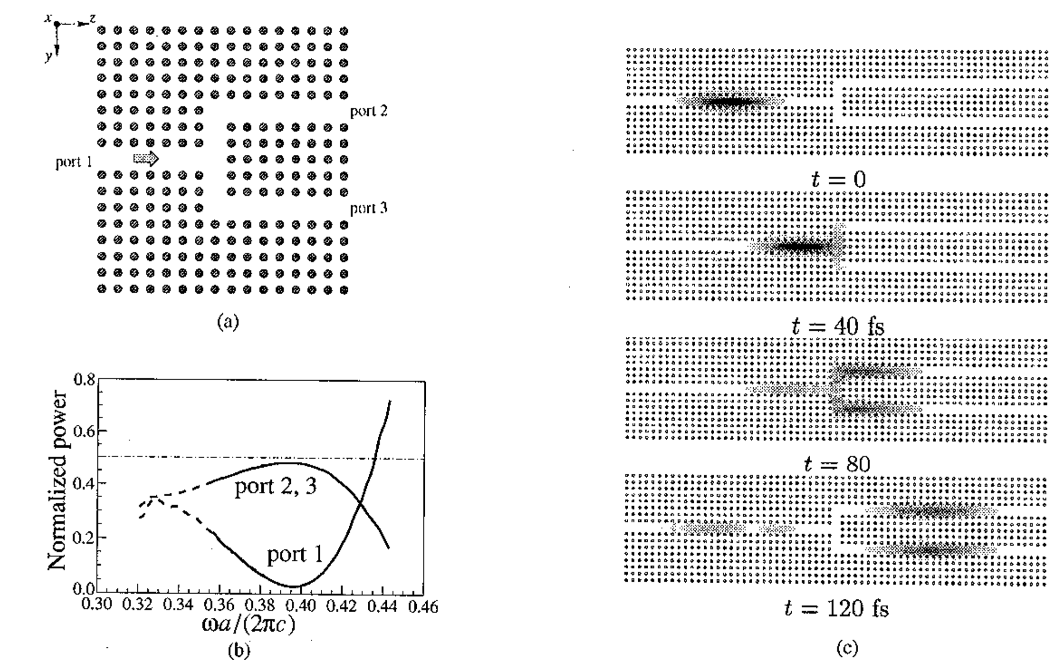

Fig. 7. T-branch with (a) structure, (b) propagation characteristics, and (c) electric field patterns.

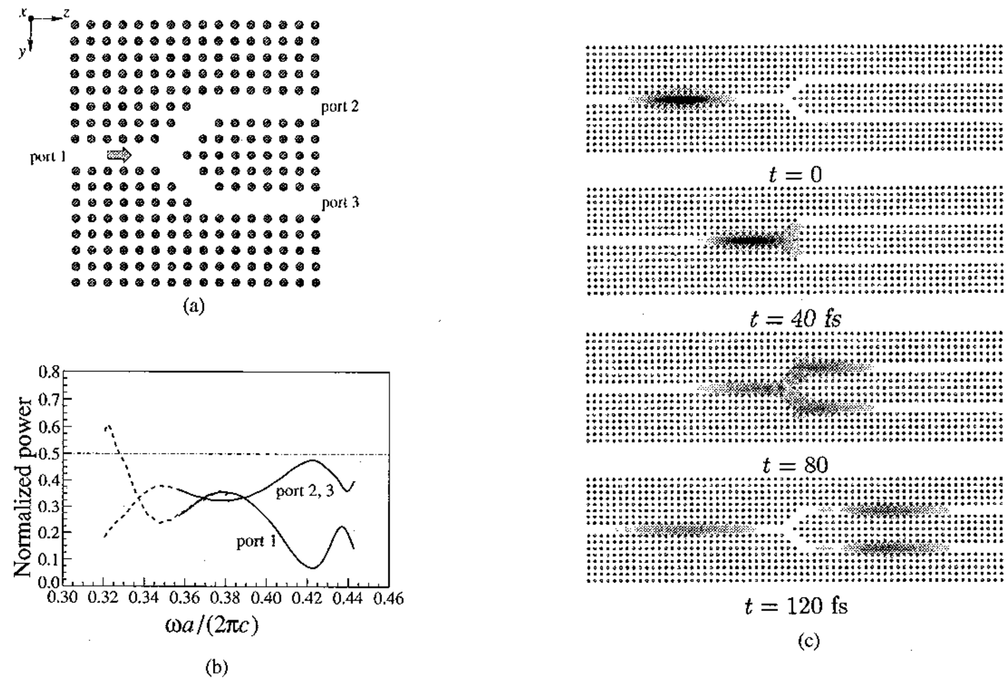

Fig. 8. Y-branch with (a) structure, (b) propagation characteristics, and (c) electric field patterns.

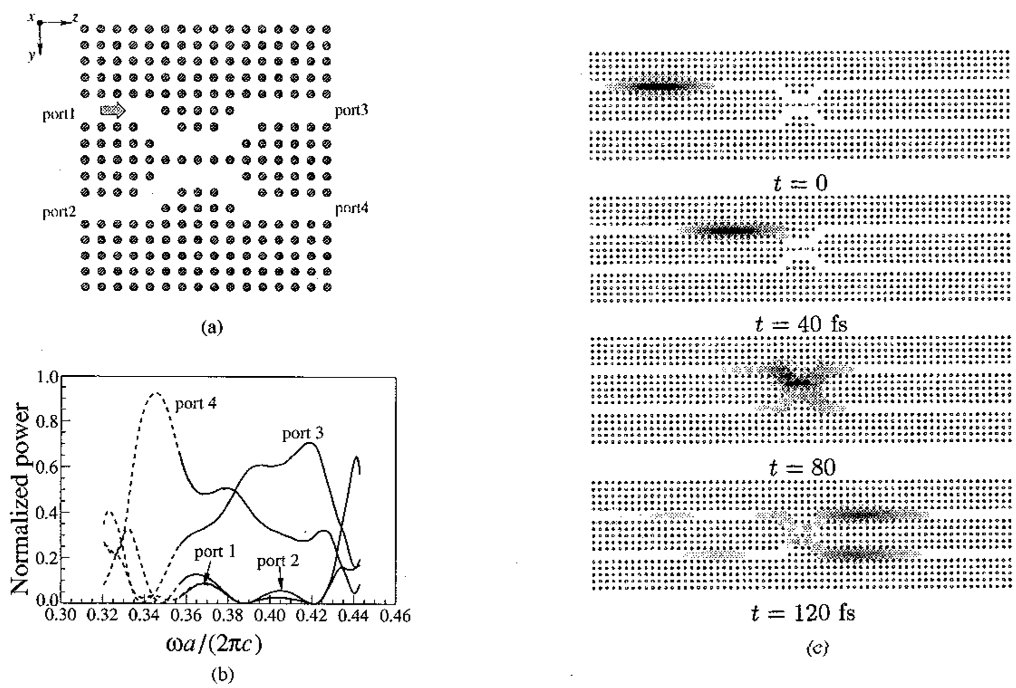

Fig. 9. Directional coupler with (a) structure, (b) propagation characteristics, and (c) electric field patterns.

1.45 μm) for the T-branch and the Y-branch are, respectively, shown in Figs. 7(c) and 8(c).

Fig. 9(a)–(c) shows, respectively, a directional coupler and its propagation characteristics, and the electric field patterns ($\lambda_0 = 1.45$ μm). It is worthy of note that a very low-loss 3-dB coupler can be realized at frequency $\omega = 0.383 \times 2\pi c/a$.

Fig. 10(a)–(c) shows, respectively, a multimode coupler, the propagatoni characteristics, and the electric field patterns ($\lambda_0 = 1.45$ μm). In this structure, equal contributions

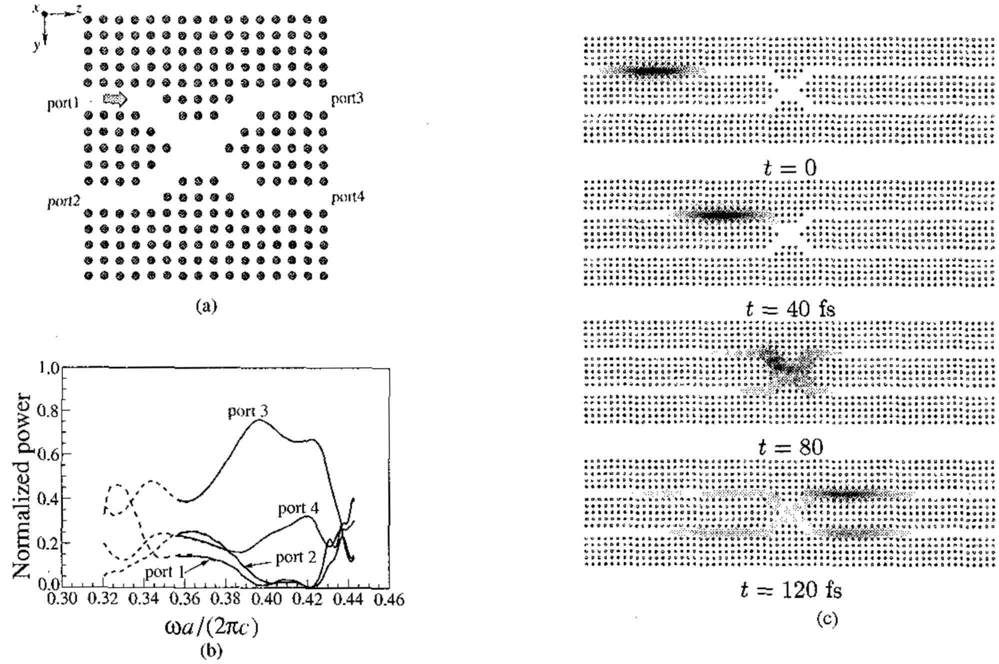

Fig. 10. Multimode coupler with (a) structure, (b) propagation characteristics, and (c) electric field patterns.

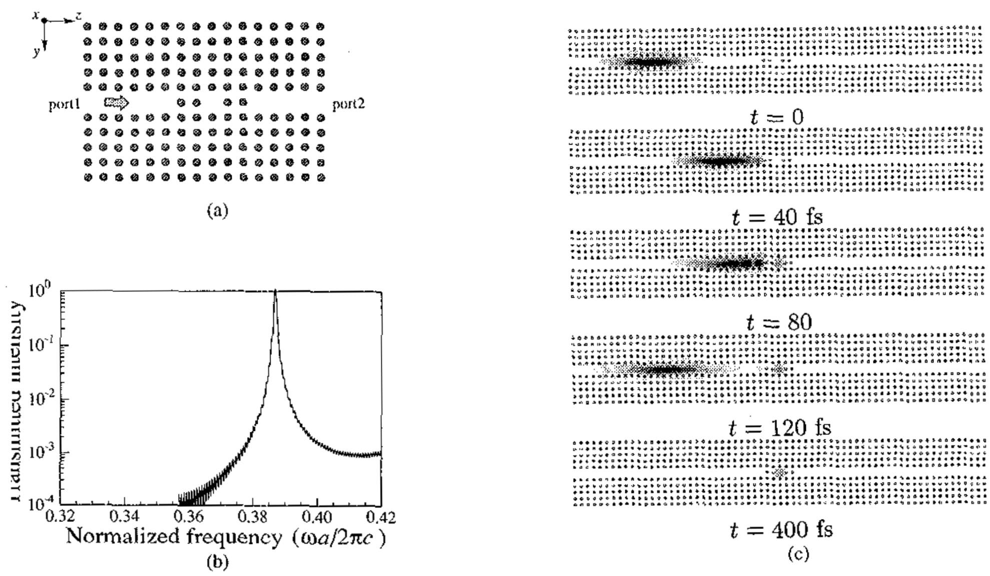

Fig. 11. Microcavity with (a) structure, (b) propagation characteristics, and (c) electric field patterns.

in ports 3 and 4 can be hardly realized at very low reflection at port 1 and transmission at port 2.

Finally, we consider single and double microcavities coupled to straight waveguides in Figs. 11(a) and 12(a). From Figs. 11(b) and 12(b), we can see that these structures can produce optical filters with sharp transmission resonances. Figs. 11(c) and 12(c) show the electric field patterns ($\lambda_0 = 1.45\ \mu$m).

V. Conclusion

A wide-band FETD-BPM using the Padé approximation was described for both TE and TM polarized pulses. To validate the present algorithm, numerical results are shown for optical gratings and are compared with the conventional FEM in frequency domain. Furthermore, various photonic crystal circuit components were simulated and those fascinating properties were demonstrated.

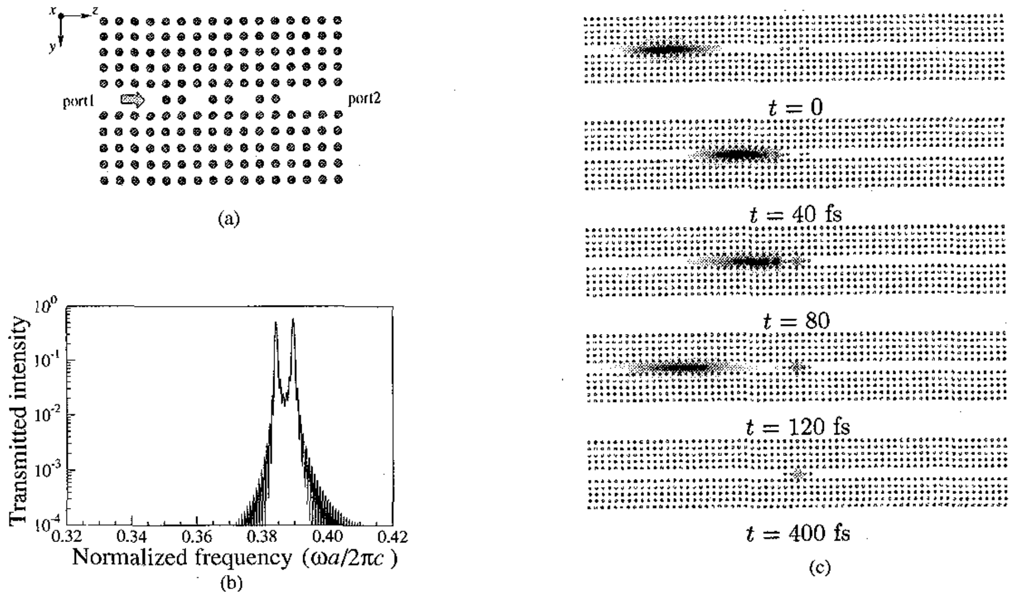

Fig. 12. Double microcavities with (a) structure, (b) propagation characteristics, and (c) electric field patterns.

A full-wave FETD-BPM for three-dimensional structures is now under consideration.

References

[1] H.-P. Nolting and R. März, "Results of benchmark tests for different numerical BPM algorithms," *J. Lightwave Technol.*, vol. 13, pp. 216–224, Feb. 1995.

[2] M. Koshiba and Y. Tsuji, "A wide-angle finite element beam propagation method," *IEEE Photon. Technol. Lett.*, vol. 8, pp. 1208–1210, Sept. 1996.

[3] Y. Tsuji, M. Koshiba, and T. Tanabe, "A wide-angle beam propagation method based on a finite element scheme," *IEEE Trans. Magnet.*, vol. 33, pp. 1544–1547, Mar. 1997.

[4] Y. Tsuji, M. Koshiba, and T. Shiraishi, "Finite element beam propagation method for three-dimensional optical waveguide structures," *J. Lightwave Technol.*, vol. 15, pp. 1728–1734, Sept. 1997.

[5] Y. Tsuji and M. Koshiba, "Finite element beam propagation method with perfectly matched layer boundary conditions for three-dimensional optical waveguides," Int. J. Numer. Modeling, to be published.

[6] G. R. Hadley, "Wide-angle beam propagation using Padé approximant operators," *Opt. Lett.*, vol. 17, pp. 1426–1428, Oct. 1992.

[7] K. S. Yee, "Numerical solution of initial boundary value problems involving Maxwell's equations," *IEEE Trans. Antennas Propag.*, vol. AP-14, pp. 302–307, May 1966.

[8] S.-T. Chu and S. Chaudhuri, "A finite-difference time-domain method for the design and analysis of guided wave optical structures," *J. Lightwave Technol.*, vol. 7, pp. 2033–2038, Dec. 1989.

[9] J. Yamauchi, M. Mita, S. Aoki, and H. Nakano, "Analysis of antireflection coatings using the FD-TD method with the PML absorbing boundary condition," *IEEE Photon. Technol. Lett.*, vol. 8, pp. 239–241, Feb. 1996.

[10] A. Mekis, J. C. Chen, I. Kurland, S. Fan, P. R. Villeneuve, and J. D. Joannopoulos, "High transmission through sharp bends in photonic crystal waveguides," *Phys. Rev. Lett.*, vol. 77, pp. 3787–3790, Oct. 1996.

[11] P.-L. Liu, Q. Zhao, and F.-S. Choa, "Slow-wave finite-difference beam propagation method," *IEEE Photon. Technol. Lett.*, vol. 7, pp. 890–892, Aug. 1995.

[12] G. H. Jin, J. Harari, J. P. Vilcot, and D. Decoster, "An improved time-domain beam propagaton method for integrated optics components," *IEEE Photon. Technol. Lett.*, vol. 9, pp. 348–350, Mar. 1997.

[13] Ü. Pekel and R. Mittra, "A finite element method frequency domain application of the perfectly matched layer (PML) concept," *Microwave Opt. Technol. Lett.*, vol. 9, pp. 117–122, June 1995.

[14] E. Yablonovitch, "Photonic band-gap structures," *J. Opt. Soc. Amer. B.*, vol. 10, pp. 293–295, Feb. 1993.

[15] J.-P. Berenger, "A perfectly matched layer for the absorption of electromagnetic waves," *J. Comput. Phys.*, vol. 114, pp. 185–200, Oct. 1994.

[16] H. A. Van der Vorst, "Bi:CGSTAB: A fast and smoothly converging variant of Bi-CG for the solution of nonsymmetric linear systems," *SIAM J. Sci. Stat. Comput.*, vol. 13, pp. 631–644, Mar. 1992.

[17] K. Hirayama, M. Koshiba, and M. Suzuki, "Finite element analysis of dielectric slab waveguide with finite periodic corrugation," *Trans. Inst. Electron. Inform. Commun. Eng.*, vol. J69, pp. 724–730, June 1986.

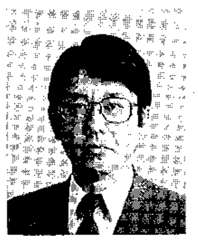

Masanori Koshiba (SM'84) was born in Sapporo, Japan, on November 23, 1948. He received the B.S., M.S., and Ph.D. degrees in electronic engineering from Hokkaido University, Sapporo, Japan, in 1971, 1973, and 1976, respectively.

In 1976, he joined the Department of Electronic Engineering, Kitami Institute of Technology, Kitami, Japan. From 1979 to 1987, he was an Associate Professor of Electronic Engineering at Hokkaido University, and in 1987, he became a Professor. He has been engaged in research on wave electronics, including microwaves, millimeter-waves, lightwaves, surface acoustic waves (SAW), magnetostatic waves (MSW), and electron waves, and computer-aided design and modeling of guided-wave devices using finite-element method, boundary element method, and beam propagation method. He is the author or coauthor of more than 200 research papers in English and more than 100 research papers in Japanese in refereed journals. He authored the books *Optical Waveguide Analysis* (New York: McGraw-Hill) and *Optical Waveguide Theory by the Finite Element Method* (Tokyo, Japan/Dordrecht, Germany: KTK Scientific Publishers/Kluwer Academic), and coauthored the books *Analysis Methods for Electromagnetic Wave Problems* (Norwood, MA: Artech House), *Ultrafast and Ultra-parallel Optoelectronics* (New York: Wiley), and *Finite Element Software for Microwave Engineering* (New York: Wiley).

Dr. Koshiba is a member of the Institute of Electronics, Information and Communication Engineers (IEICE) of Japan, the Institute of Electrical Engineers of Japan, the Institute of Image Information and Television Engineers of Japan, the Japan Society for Simulation Technology, the Japan Society for Computational Methods in Engineering, the Japan Society of Applied Electromagnetics and Mechanics, the Japan Society for Computational Engineering and Science, and the Applied Computational Electromagnetics Society (ACES). In 1987, 1997, and 1999, he was awarded the Excellent Paper Awards from the IEICE, respectively, and in 1998, he was awarded the Electronics-Society Award from the IEICE.

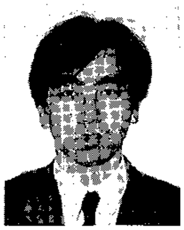

Yasuhide Tsuji (M'97) was born in Takikawa, Japan, on December 31, 1967. He received the B.S., M.S., and Ph.D. degrees in electronic engineering from Hokkaido University, Sapporo, Japan, in 1991, 1993, and 1996, respectively.

In 1996, he joined the Department of Applied Electronic Engineering, Hokkaido Institute of Technology, Sapporo, Japan. Since 1997, he has been an Associate Professor of Hokkaido University, Sapporo, Japan. He has been engaged in research on wave electronics.

Dr. Tsuji is a member of the Institute of Electronics, Information and Communication Engineers (IEICE) of Japan. In 1997 and 1999, he was awarded the Excellent Paper Awards from the IEICE, and in 1999, he was awarded the Young Scientist Award from the IEICE.

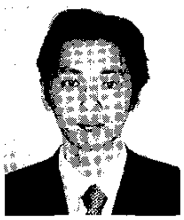

Masafumi Hikari was born in Ichihara, Japan, on August 3, 1973. He recieved the B.S. and M.S. degrees in electronic engineering from Hokkaido University, Sapporo, Japan, in 1997, and 1999, respectively.

He is currently working at Hitachi, Ltd., Tokyo, Japan.

Mr. Hikari is a member of the Institute of Electronics, Information and Communication Engineers (IEICE) of Japan.